TISSUE ENGINEERING: Part A
Volume 20, Numbers 21 and 22, 2014

DOI: 10.1089/ten.tea.2014.0011

Barrier Properties of an N/TERT-Based Human Skin Equivalent

Vincent van Drongelen, MSc,[1,2] Mogbekeloluwa O. Danso, MSc,[1] Aat Mulder,[2] Arnout Mieremet, BSc,[1] Jeroen van Smeden, PhD,[1] Joke A. Bouwstra, PhD,[1] and Abdoelwaheb El Ghalbzouri, PhD [2]

Human skin equivalents (HSEs) can be considered a valuable tool to study aspects of human skin, including the skin barrier, or to perform chemical or toxicological screenings. HSEs are three-dimensional skin models that are usually established using primary keratinocytes and closely mimic human skin. The use of primary keratinocytes has several drawbacks, including a limited *in vitro* life span and large donor–donor variation. This makes them less favorable for *in vitro* toxicity screenings. Usage of an established keratinocyte cell line circumvents these drawbacks and enables the generation of easy-to-generate and reproducible HSEs, which can be used for pharmacological and/or toxicological screenings. For such screenings, a proper barrier function is required. In this study, we investigated the barrier properties of HSEs established with the keratinocyte cell line N/TERT (N-HSEs). N-HSEs showed comparable tissue morphology and expression of several epidermal proteins compared with HSEs established with primary keratinocytes. Our results clearly demonstrate that N-HSEs not only contain several stratum corneum (SC) barrier properties similar to HSEs, including the presence of the long periodicity phase and a comparable SC permeability, but also show some differences in lipid composition. Nonetheless, the similarities in barrier properties makes N/TERT cells a promising alternative for primary keratinocytes to generate HSEs.

Introduction

The main function of human skin is to act as a barrier, thereby preventing excessive water loss and protecting against harmful substances and pathogens. The stratum corneum (SC) is the outermost epidermal layer and is the principle site of the skin barrier. The SC is composed of corneocytes embedded in a hydrophobic lipid matrix, mainly composed of ceramides (CERs), free fatty acids (FFAs), and cholesterol (CHOL). These lipids are organized in stacked lipid layers, referred to as a lamellar phase, oriented parallel to the skin surface.[1–3] SC from native human skin contains two lamellar phases, the long periodicity phase (LPP) and the short periodicity phase with a repeat distance of ~13 and ~6 nm, respectively.[4] Within these lipid lamellae, the lipids are organized in an orthorhombic (very dense), hexagonal (dense), or liquid (loose) packing (Supplementary Fig. S1; Supplementary Data are available online at www.liebertpub.com/tea).[5,6]

To study aspects of skin biology and skin barrier, various model systems, in particular animal models, are currently used. However, animal skin displays different epidermal morphology compared with human skin; for example, mouse skin has generally two to three viable cell layers, while human skin has seven to eight cell layers. In addition, mouse skin displays higher percutaneous absorption compared with human skin, thereby limiting its use for topical drug-delivery studies.[7] Therefore, data obtained from animal studies are difficult to extrapolate to *in vivo* human skin. Furthermore, there is an increasing social and political pressure to reduce animal usage and to implement alternatives.[8–11] An attractive alternative is the use of *in vitro* human skin equivalents (HSEs). These HSEs are three-dimensional culture models that are usually established by seeding primary keratinocytes onto a dermal substrate and culturing them at the air–liquid interface. These HSEs have been shown to have fairly similar morphology, expression of differentiation markers, and lipid properties compared with native human skin.[12–15]

However, usage of primary keratinocytes has several disadvantages, for example, limited availability of fresh skin, limited *in vitro* lifespan, and, in particular, the large donor–donor variation.[16] By using an established immortalized keratinocyte cell line that can be kept in culture for prolonged time, such limitations can be circumvented. This enables the possibility to generate a robust and reproducible

[1]Gorlaeus Laboratories, Department of Drug Delivery Technology, Leiden Academy Centre for Drug Research, Leiden University, Leiden, The Netherlands.
[2]Department of Dermatology, Leiden University Medical Centre, Leiden, The Netherlands.

HSE that is desirable for pharmacological and/or toxicological screening purposes. The presence of a competent skin barrier is a prerequisite for HSEs when used for topical application studies (e.g., toxicological screening).

In this study, we demonstrate that N/TERT-based HSEs (N-HSEs) show normal epidermal morphogenesis and the formation of a SC which displays a lamellar and lateral lipid organization and permeability comparable to that of HSEs. However, N-HSEs displayed some differences in the lipid composition. Our results demonstrate that N/TERT cells can be used in addition to primary keratinocytes to generate HSEs, and that these N-HSEs might, therefore, be a promising alternative for toxicological safety screening.

Materials and Methods

Cell culture

Primary human keratinocytes and dermal fibroblasts were obtained from surplus skin from adult donors undergoing mammary or abdominal surgery and were established and cultured as described earlier.[17] Skin was handled according to the declaration of Helsinki principles and collected after informed written consent had been obtained. Primary keratinocytes were stored in liquid nitrogen until usage for generation of HSEs. For all experiments, primary keratinocytes (passage 1 or 2) and fibroblasts (passage 2 till 5) from different donors were used for generation of HSEs.

The N/TERT keratinocyte cell line was purchased from Harvard Medical School and cultured under low confluency ($<40\%$) in keratinocyte serum-free medium (Invitrogen, Carlsbad, CA). The N/TERT cell line was originally generated by overexpression of telomerase in primary keratinocytes that lacked expression of cell cycle regulatory protein $p16^{ink4a}$.[18]

Dermal equivalents

Dermal equivalents were generated as described earlier.[19] In short, 1 mL of cell-free collagen (1 mg/mL) solution was pipetted into a six-well-filter insert (Corning Life Sciences, Tewksbury MA). After polymerization, 3 mL of fibroblast-populated (0.4×10^5 fibroblasts/mL) collagen (2 mg/mL) solution was pipetted onto the previous collagen layer. After polymerization, the dermal equivalents were submerged in medium consisting of Dulbecco's modified Eagle's medium, 5% fetal calf serum, and 1% penicillin/streptomycin. The medium was refreshed twice a week. The dermal equivalents were cultured under submerged conditions for 3–4 days before seeding of keratinocytes.

Generation of HSEs

HSEs and N-HSEs were generated by seeding 0.5×10^6 primary keratinocytes (mixture of two donors in a 1:1 ratio) or N/TERT cells onto the dermal equivalent, respectively, as described elsewere.[19,20] Details are given in the Supplementary Materials and Methods section.

Morphological and immunohistochemical analysis

HSEs were fixed in 4% formaldehyde and embedded in paraffin. Morphological analysis was performed on 5 μm sections through hematoxylin and eosin staining. Immunohistochemical analysis was performed using the streptavidin-biotin-peroxidase system (GE Healthcare, Buckinghamshire, United Kingdom), according to the manufacturer's instructions. Staining's were visualized with 3-amino-9-ethylcarbazole (AEC), counterstained with hematoxylin, and sealed with Kaiser's glycerin. Primary and secondary antibodies are given in Table 1 of the Supplementary Materials and Methods section. For the collagen IV staining, a protease treatment using a 0.025% protease solution (Sigma, Zwijndrecht, The Netherlands) was done before incubation with the primary antibody.

Estimation of proliferation index

To estimate the proliferation index, the number of Ki67-positive nuclei in a total number of 100 basal cells ($\times100\%$) was determined at three locations per slide for four different experiments. An independent researcher performed counting of the Ki67-positive cells.

Determination of the number of SC layers

To determine the number of SC layers, 5 μm sections from snap-frozen HSEs were cut and stained with a 1% (w/v) safranin (Sigma) solution for 1 min. To enable corneocyte swelling, sections were incubated for 20 min with a 2% (w/v) KOH solution. Images of the sections were taken, and the number of layers was counted in at least six locations covering the full length of the N-HSEs or HSEs. This was performed for four independent experiments.

SC isolation

The SC from both HSE types was isolated as described earlier.[21,22] Briefly, (N-) HSEs were incubated overnight on filter paper with 0.1% trypsin in 4°C. After a 30 min incubation at 37°C, the SC was mechanically separated from the N-HSEs and HSEs and subsequently washed with 1 μg/mL trypsin inhibitor (Sigma) and demineralized water. SC samples were air dried at room temperature and stored under Argon gas over silica gel in the dark.

Fourier transformed infrared spectroscopy and small-angle X-ray diffraction

Fourier transform infrared spectroscopy (FTIR) and small-angle X-ray diffraction (SAXD) were performed as described earlier.[22] In short, SC samples were hydrated at room temperature for 24 h in a 27% (w/v) NaBr solution before FTIR and SAXD measurements.

FTIR spectra were obtained using a Varian 670-IR FTIR spectrometer (Agilent technologies, Santa Clara, CA), equipped with a broad-band mercury cadmium telluride detector that was cooled with liquid nitrogen.

SAXD measurements were performed at the European Synchrotron Radiation Facility (ESRF, Grenoble) at station BM26B. All FTIR and SAXD measurements were performed with three SC samples of both HSE types. Details with regard to FTIR and SAXD measurements are given in the Supplementary Materials and Methods section.

High-performance thin-layer chromatography lipid analysis

The SC lipids were extracted according to a modified Bligh and Dyer procedure as described elsewhere.[23] Details

are given in the Supplementary Materials and Methods section. Extracted SC lipids were quantified using high-performance thin-layer chromatography (HPTLC). The used solvent system to separate the lipids is described elsewhere.[22] For quantification, co-chromotography of serial dilutions of each of the standards was done as described earlier.[23] The standards consisted of CHOL, palmitic acid, stearic acid, arachidic acid, tricosanoic acid, behenic acid, lignoceric acid, cerotic acid, and CER EOS, NS, NP, EOP, AS, and AP. CER nomenclature according to the terminology of Masukawa *et al.* and Motta *et al.*[24,25] Details about CER nomenclature and quantification are provided in the Supplementary Materials and Methods section. Quantification was performed using lipid extracts from two different experiments.

Liquid chromatography mass spectrometry for FFA lipid analysis

The CERs in the pooled lipid extracts of the HSEs and N-HSEs were analyzed using an Alliance 2695 HPLC (Waters, Milford, MA) coupled to a TSQ Quantum MS (Thermo Finnigan, San Jose, CA) measuring in APCI mode as described elsewere.[26]

The separation of FFAs was achieved using a LiChroCART Purospher STAR analytical column ($55 \times 2\,\mu m$ i.d.; Merck, Darmstadt, Germany) under a 0.6 mL/min flow rate with a gradient system from acetonitrile/H_2O to methanol/heptane. The ionization mode and scan range was altered to negative mode and 200–600 a.m.u., respectively. The total lipid concentration of all samples was around 1 mg/mL and for the analysis of FFAs, the injection volume was set to 10 μL. Quantification of FFAs was performed using lipid extracts of SC from two experiments for both HSE types.

Permeability studies

In vitro permeation studies were performed with butyl para-aminobenzoic acid (butyl-PABA) using Permegear in-line diffusion cells (Bethlehem, PA) with a diffusion area of $0.28\,cm^2$ as described earlier, with small adjustments.[21] The donor compartment was filled with 1.5 mL butyl-PABA solution (50 μg/mL butyl-PABA) in acetate buffer (pH 5.0). The acceptor compartment consisted of phosphate-buffered saline (pH 7.4), which was perfused at a flow rate of 1.5 mL/h. Permeability studies were performed with at least six SC sheets of HSE and N-HSE type.

Statistical analysis

Statistical significance was determined using the two-tailed Student's *t*-test. The permeability studies were analyzed using one-way ANOVA.

Results

N/TERT-based HSEs (N-HSEs) and primary keratinocyte HSEs show similar epidermal morphogenesis

To evaluate whether N/TERT cells can be used for the generation of HSEs and whether they display similar epidermal morphogenesis compared with HSEs generated with primary keratinocytes, we have examined the morphology, expression of differentiation proteins, and the proliferation in (N-)HSEs that have been cultured for 14 days at the air–liquid interface. As shown in Figure 1, N-HSEs display all the epidermal strata, including the SC. A normal basement membrane was formed as shown by the expression of collagen type IV at the dermal–epidermal junction (Fig. 1A). Immunohistochemical analyses for keratin 10 (K10), filaggrin, and loricrin showed that N-HSEs display expression of these proteins, comparable to that of HSEs (Fig. 1A).

N-HSEs also expressed the desquamation-related proteins kallikrein 5 (KLK5) and lympho-epithelial Kazal type-related inhibitor (Lekti) comparable to HSEs generated with primary keratinocytes (Fig. 1A). In N-HSEs, generally four to five viable epidermal cell layers were observed compared with seven to eight cell layers observed in HSEs. The proliferation index of N-HSEs was not significantly different compared with HSEs (Fig. 1B). Finally, we determined the thickness of the SC by using a saffranin red staining. No significant differences in the number of SC layers between the N-HSEs and HSEs were found (Fig. 1C).

SC lipid composition of N-HSEs displays similarities to HSEs

After evaluation of the epidermal morphogenesis of N-HSEs, we continued with the evaluation of the SC barrier properties. Since the extracellular lipid matrix is regarded to be the main route for penetration, we mainly focused on lipid composition, lipid organization, and SC permeability.

HPTLC can be used to detect nine CER subclasses. This method revealed that N-HSEs displayed the presence of all nine CERs, CHOL, and FFAs, comparable to HSEs with (Fig. 2A). Before and after lipid extraction, dry SC was weighted from which the percentage of lipids present in dry SC was calculated. As shown in Figure 2B, the level of lipids in SC from N-HSEs and HSEs was comparable (Fig. 2B). Quantification revealed that the relative amounts for CERs, CHOL, and FFA were similar between N-HSEs and HSEs (Fig. 2C). The levels of most CER subclasses in HSE and N-HSE were similar; however, some differences were also noticed. CERs AS/NH was more pronounced in the N-HSEs than in HSEs, while the presence of CER AP was reduced in N-HSEs compared with HSEs (Fig. 2D). Furthermore, the ratio between all ω-hydroxy CERs (EO CERs) and the other ceramide subclasses (non-EO CERs) was lower in the N-HSEs (Fig. 2E).

Using liquid chromatography/mass spectrometry (LC/MS), we observed the presence of all 12 CERs in the SC of N-HSEs as observed in the LC/MS profile of HSE (Fig. 3A, B). However, we also noticed some changes in the CER composition. The peak intensities in the LC/MS chromatogram for the polar CERs (e.g., AP, EOP, and NP) in the N-HSE were less present compared with the LC/MS chromatogram for the HSE, confirming the HPTLC results (Fig. 3A, B).

The range of the CER chain length distribution is similar in both HSEs and N-HSEs (Fig. 3A, B).

In addition, LC/MS was used to quantify the levels of saturated FFAs, mono-unsaturated FFA (MUFAs), and hydroxy-FFAs. We observed a comparable level of saturated FFAs between the N-HSEs and the HSEs; while in N-HSE, the MUFA content was increased at the expense of the OH-FAs (Fig. 3E).

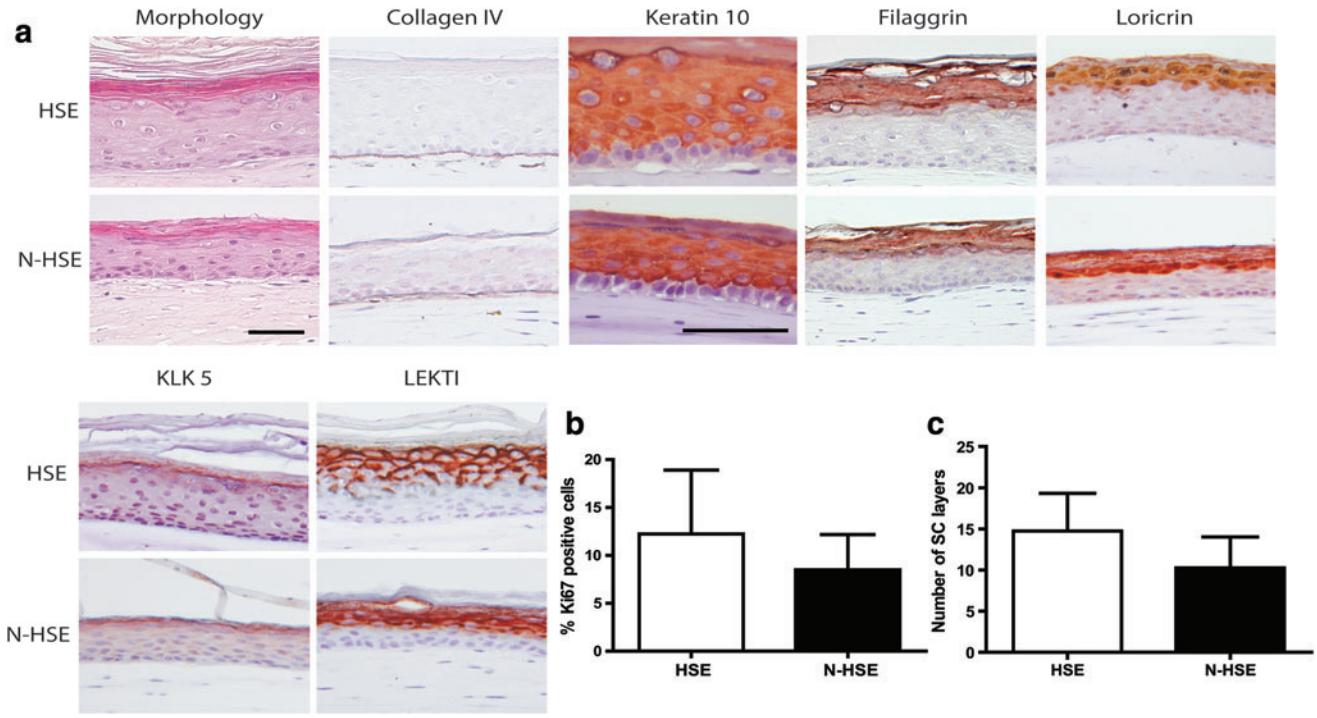

FIG. 1. **(a)** Cross-sections of hematoxilin and eosin and immunohistochemical staining for collagen type IV, early (keratin 10 [K10]) and late (filaggrin, loricrin) differentiation markers, and for desquamation-related proteins kallikrein 5 (KLK5), Lekti. **(b)** Graph represents the proliferation index of human skin equivalents (HSEs) and N-HSEs. **(c)** Graph represents the stratum corneum (SC) thickness in terms of number of SC layers. Data represent the mean + SD of four experiments. Scale bars represent 50 μm. Color images available online at www.liebertpub.com/tea

Besides the subclass levels, the chain length distribution was also examined. Based on the number of carbon (C) atoms, FFAs in the SC can be divided in long-chain fatty acids (LCFA, with chain length varying between C16 and C21) and very long chain fatty acids (VLCFA, chain length between C22 and C38). The levels of the LCFAs and VLCFAs did not vary between the N-HSEs and HSEs (Fig. 3F). Quantification of the individual FFAs is provided in Supplementary Data (Supplementary Fig. S2).

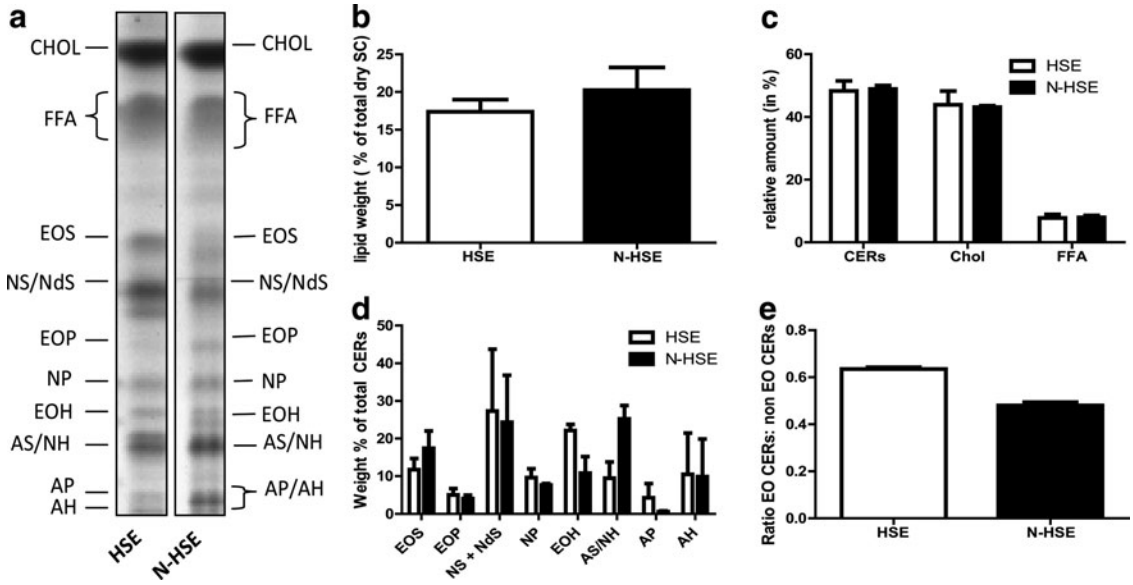

FIG. 2. SC lipid composition analysis of HSEs generated with primary keratinocytes (HSE) and N-HSEs. **(a)** Lipid profiles of HSEs and N-HSEs. **(b)** Total level of lipids present in dry SC. **(c)** Relative weight % of the different lipid classes, ceramides (CER), cholesterol (CHOL), and free fatty acids (FFA). **(d)** Relative level of CERs in weight % of total CERs. **(e)** Ratio between the EO CER and non-EO CER. Data represent mean + SEM from two independent experiments.

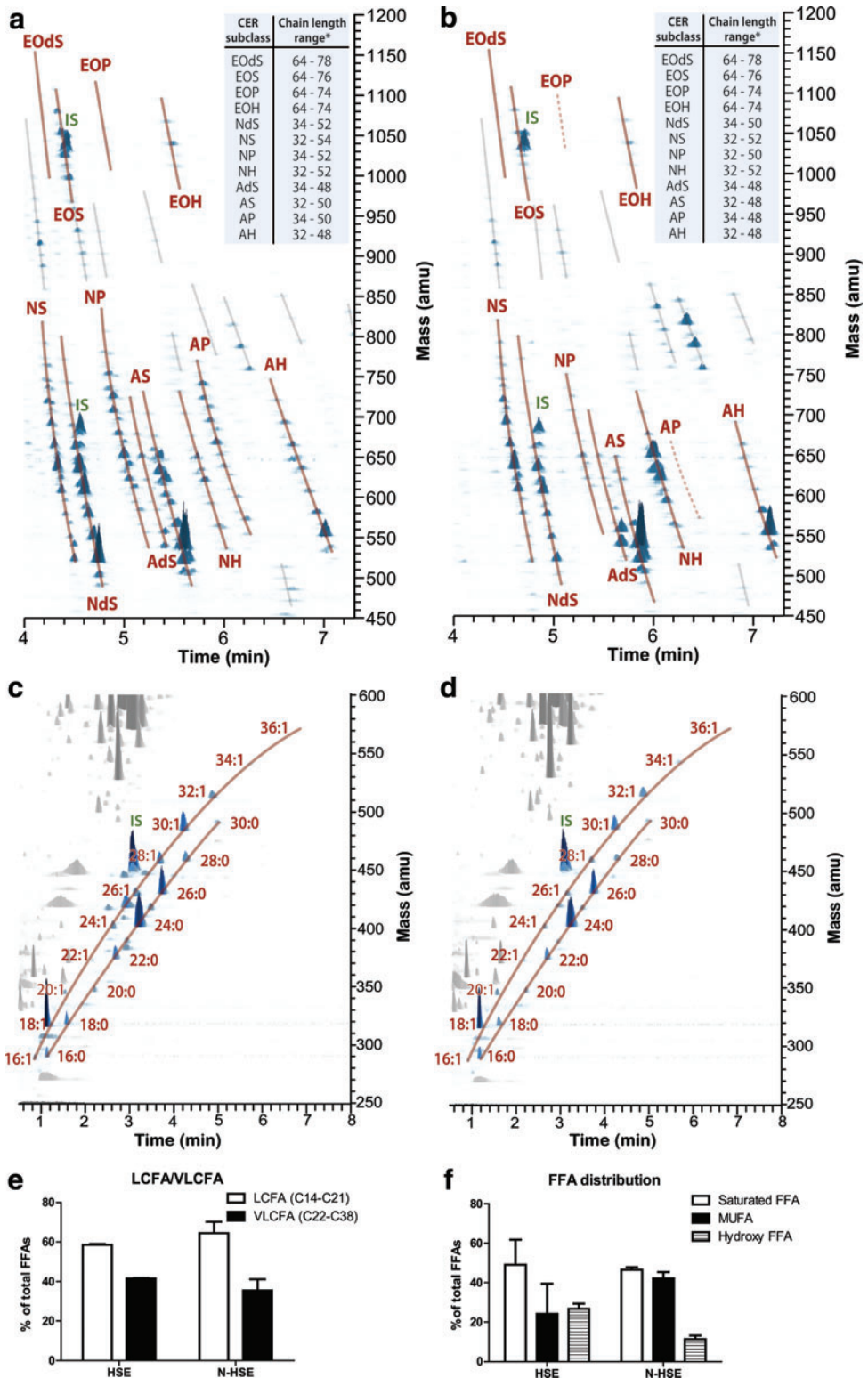

FIG. 3. Three-dimensional multi-mass liquid chromatography/mass spectrometry (LC/MS) chromatogram showing the presence of the 12 CER subclasses in SC from **(a)** HSEs and **(b)** N-HSEs. CERs are indicated with a continuous line. CERs with reduced peak intensity are indicated with a dotted line. Unknown lipid species are indicated with a gray line. Three-dimensional multi-mass LC/MS chromatogram showing the saturated FAs, and mono-unsaturated FFA (MUFA) in the SC from **(c)** HSE and **(d)** N-HSEs. **(e)** Distribution of the different FFA subclasses in SC of HSE and N-HSE. **(f)** Long-chain fatty acid (LCFA)/very long-chain fatty acid (VLCFA) distribution in SC of HSEs and N-HSEs. Data represent mean + SEM of two independent experiments. * Chain lengths based on number of carbon atoms. Color images available online at www.liebertpub.com/tea

N-HSEs and HSEs show similar lateral lipid organization

After the evaluation of the lipid composition, we assessed the lipid organization. The lateral packing in the SC of the N-HSEs and HSEs was examined using FTIR. The lateral packing can be determined by monitoring the CH_2 rocking vibrations in the FTIR spectrum. When lipids are in a crystalline dense orthorhombic packing, the CH_2 rocking band consists of two vibrations at 719 and 730 cm^{-1}, whereas a hexagonal less dense lateral packing results in a single vibration at 719 cm^{-1}. A detailed explanation of FTIR and its usage for the evaluation of the lateral packing in the SC of HSEs is described in detail elsewhere.[22] As

shown in Figure 4, both N-HSEs and HSEs displayed the presence of one peak around 719 cm^{-1}, indicating a hexagonal lateral packing (Fig. 4).

To evaluate at which temperatures the ordered phase (orthorhombic or hexagonal packing) transforms into a liquid phase, the CH_2 symmetric stretching vibrations were assessed. This provides information about the conformational disorder of the lipids. When organized in an ordered packing, the carbon chains are fully extended, resulting in CH_2 symmetric stretching wavenumbers that are below 2850 cm^{-1}. In a liquid phase, the conformational disordering is high, resulting in CH_2 symmetric stretching vibrations of around 2852–2854 cm^{-1}. The lipids in the SC of both HSEs displayed similar conformational disordering illustrated by a CH_2 stretching frequency of 2850.1 cm^{-1} (HSEs) and 2850.3 cm^{-1} (N-HSE) (Fig. 4, table).

FTIR measures the order-disorder transition in a temperature range between 0°C and 90°C; therefore, the midpoint temperature of this transition could be determined for both N-HSEs and HSEs. The table in Figure 4 shows that this midpoint temperature of the steep shift in CH_2 symmetric stretching frequency of the order–disorder transition occurs at similar temperatures in both HSE types (Fig. 4).

SC of N-HSEs display the presence of the LPP

The lamellar lipid organization in the SC of HSEs can be determined by SAXD. From the position of diffraction peaks, the presence of lamellar phases and their repeat distance can be determined. As shown in Figure 5, the SAXD profiles display three diffraction peaks, representing the first-, second-, and third-order diffraction peaks of a

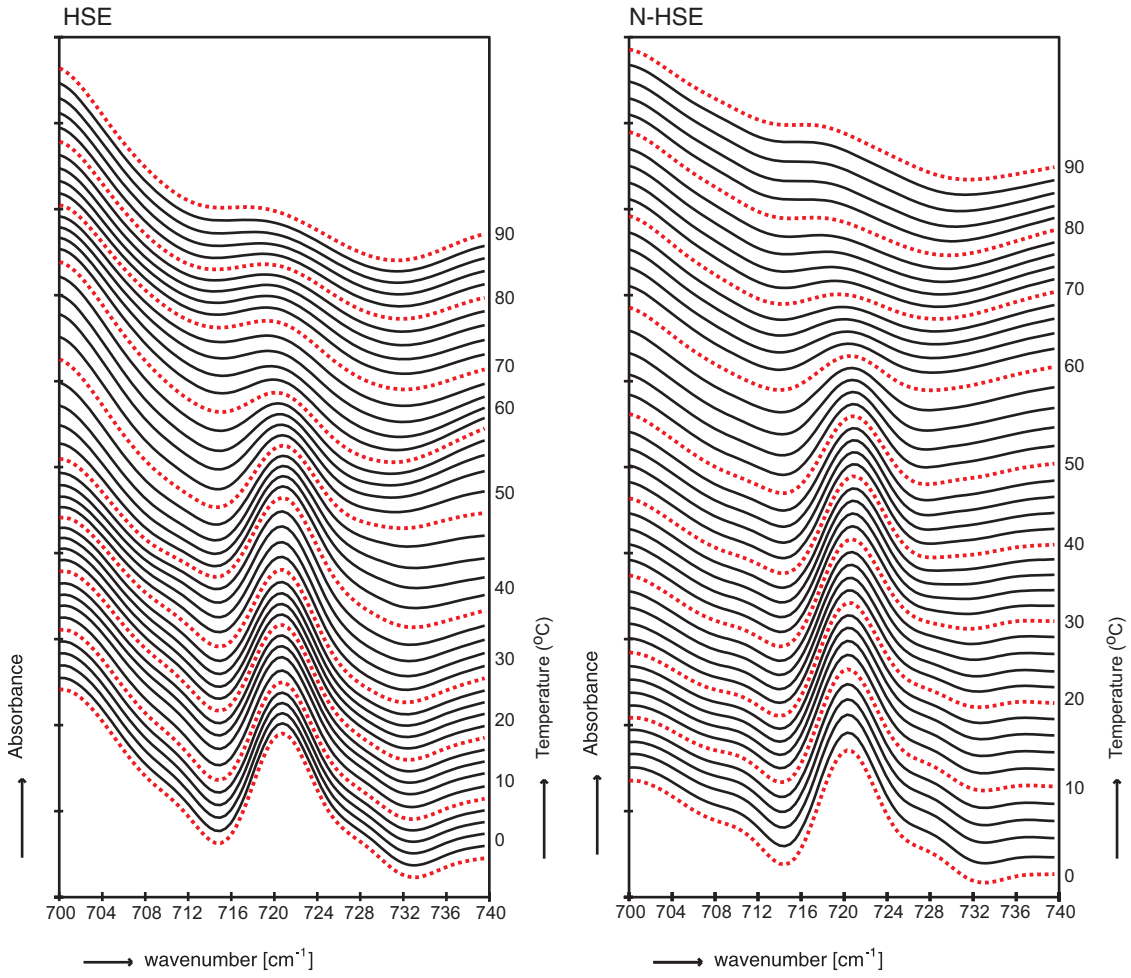

HSE type	Midpoint Order-Disorder Transition	Symetric stretching (cm^{-1}) at 32°C
HSE	58 ± 2°C	2850,1 ± 0
N-HSE	57,3 ± 2,3°C	2850,3 ± 0,2

FIG. 4. Representative rocking vibrations over a temperature range from 0°C to 90°C in the Fourier transform infrared spectroscopy (FTIR) spectrum from SC of HSEs or N-HSEs. Both HSE types form hexagonal lateral packing in the SC illustrated with one peak at 719 cm^{-1}. Table: The midpoint order–disorder transition temperature and the symmetric stretching for both HSE types. Data represent the mean ± SD of three experiments. For a detailed explanation about SC lipid organization and FTIR, see Thakoersing *et al.*[22] Color images available online at www.liebertpub.com/tea

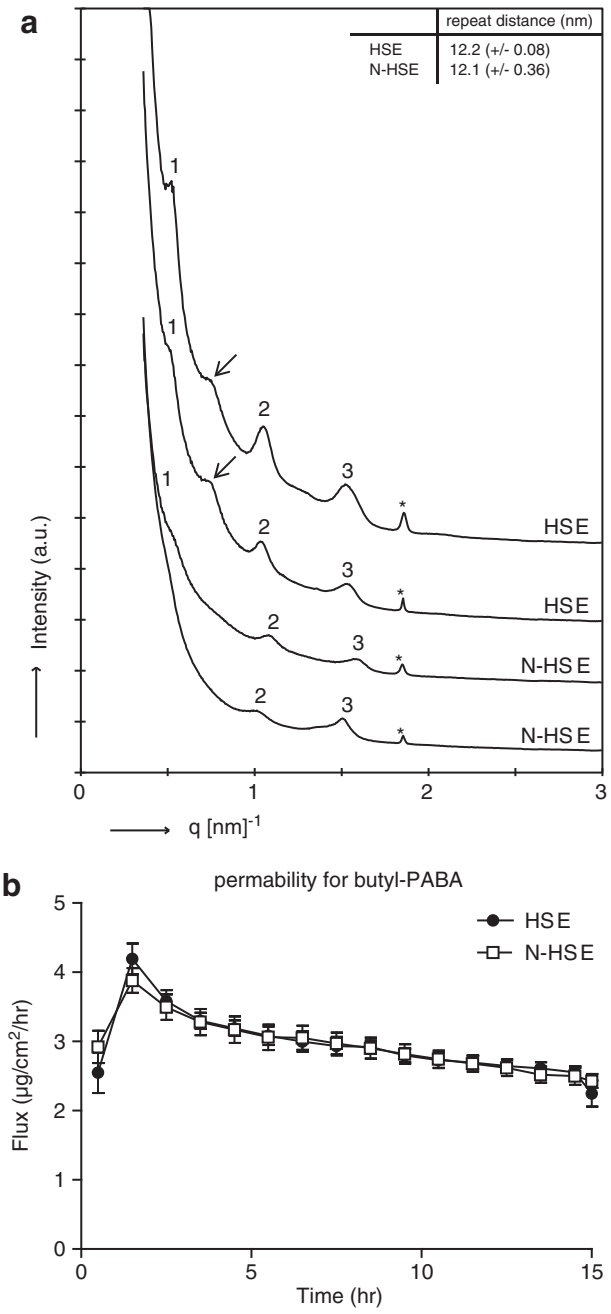

FIG. 5. **(a)** Two representative small-angle X-ray diffraction profiles for the HSE and N-HSE are shown. The first-, second-, and third-order diffraction peaks are indicated by 1, 2, and 3, respectively, and the * indicates phase-separated crystalline CHOL. Both HSEs and N-HSE display the first-, second-, and third-order diffraction peaks, indicating the presence of the long periodicity phase. The arrow indicates an additional peak that was sometimes observed in the HSEs. The data represent the mean ± SD of three experiments. **(b)** Diffusion profiles for diffusion of butyl-PABA through the SC of HSEs and N-HSEs. The data represent the mean ± SEM of at least six measurements.

lamellar phase with a repeat distance of 12.2 (±0.08) nm for SC for HSE and 12.1 (±0.34) nm for SC in N-HSE (Fig. 5A). The peak intensity of the N-HSEs was generally lower compared with that of the HSEs. In addition to the first-, second-, and third-order diffraction peaks, an additional peak was sometimes observed in the SAXD profile of the HSEs, which might indicate the presence of phase-separated EO CERs (Fig. 5A, indicated with an arrow).[27]

SC permeability for butyl-PABA is similar for N-HSEs and HSEs

To evaluate the barrier function of the SC of N-HSEs and that of HSE, an *in vitro* permeability study was performed to determine the flux of butyl-PABA through the SC. As shown in Figure 5B, the flux of butyl-PABA through the SC of both HSEs is comparable, indicating that the permeability of the SC for butyl-PABA is similar for both HSEs and N-HSEs (Fig. 5B).

Discussion

For *in vitro* topical application studies, reproducible HSEs with a competent barrier can be used as an alternative for animal studies. To reduce donor–donor variations and to circumvent the limited *in vitro* lifespan of primary keratinocytes, epithelial cell lines can be a useful alternative. Unfortunately, not many epithelial cell lines can be used for the generation of HSEs.[28,29]

Recently, the commercially available cell line NIKS® has been shown to form a fully stratified epidermis when cultured on a fibroblast populated dermal substrate and shown to be applicable for toxicological assays (StrataTest; Stratatech, Madison, WI).[30,31] These skin models have been shown to display a barrier function as measured by skin surface electrical impedance. To the best of our knowledge, no in-depth studies have been performed so far while focussing on the SC barrier properties of HSEs established with N/TERT cells. In this study, we compared epidermal morphogenesis and barrier function of our in-house full-thickness HSEs established with primary keratinocytes or with N/TERT cells.

Morphology and protein expression

Our in-house HSEs established with primary keratinocytes have been shown to have features comparable to those seen *in vivo*, in terms of morphology and differentiation.[22] Furthermore, in the most recent publication in which different commercial available HSEs have been evaluated, the EpiDerm skin model was shown to have comparable morphology, lipid profiles, and the presence of the LPP in the SC, similar to our in-house HSEs.[22,32] N-HSEs showed expression and localization of differentiation markers, K10, filaggrin, and loricrin, and of proteins involved in desquamation, Lekti and KLK5, similar to HSEs established with primary keratinocytes. Formation of a proper basement membrane was confirmed by the presence of collagen type IV at the dermal–epidermal junction. These results indicate that full-thickness HSEs established with N/TERT cells have an epidermal morphogenesis comparable to that of HSEs generated with primary keratinocytes, and are in line with previously published results in which positive staining

for K10 and involucrin of differentiating monolayer N/TERT immortalized cells was shown.[18]

However, we observed a difference in epidermal thickness and in number of viable cell layers. While the HSEs contained seven to eight viable cell layers, the N-HSE had four to five viable cell layers. This might be caused by the immortalization in the N/TERT cells or due to the usage of a mixture of two primary keratinocyte donors for the generation of the HSEs.

Barrier properties

The main focus of this study was the evaluation of the barrier properties of N-HSEs. The results presented here indicate that N-HSEs and HSEs display barrier properties that are similar to a large extent. Evaluation of the lateral packing showed that the lipid density and the conformational ordering of the SC lipids were comparable. More importantly, the SC lipids in N-HSEs form the LPP, comparable to the lipid organization in SC of HSEs. Previously, it has been shown that presence of the LPP is an important factor for a proper barrier function.[21,33] However, some differences were also observed. A reduced peak intensity was observed in the SAXD profile of N-HSEs, which might be caused by less-ordered lipid lamellae. With regard to the lipid composition, HPTLC and LC/MS showed that N-HSEs and HSEs display the presence of all 12 CER subclasses, although the presence of some CERs, in particular CER AP, were reduced in the N-HSEs. In addition, saturated FFAs, MUFAs and hydroxy FFAs were present in both the N-HSEs and HSEs. However, differences were observed in the level of MUFA's and hydroxy FFAs. The range of the FFA and CER chain length distribution of N-HSEs was similar to HSEs. These observed differences in lipid composition in the SC from N-HSEs in terms of CER profile did not affect the permeation of N-HSEs for the lipophilic compound butyl-PABA, which has previously been described for its usage in SC permeability studies.[21]

Conclusion

In this study, we demonstrate that the N/TERT cell line is able to form a proper epidermal skin barrier when used for the generation of HSEs. The differences that were found in the SC lipid composition did not affect the barrier function in terms of SC permeability for butyl-PABA. A full characterization of the SC permeability by using a range of compounds with varying lipophilicity is a subject for future research.

Despite the discrepancy between *in vitro* HSEs and *in vivo* skin which were published earlier,[22] the results presented in this study demonstrate that the N/TERT cell line can be used as an alternative to primary keratinocytes to generate HSEs. Usage of N/TERT cells results in a reproducible, robust, and easy-to-establish *in vitro* skin model. However, their applicability for pharmacological, chemical, and toxicological (safety) testing should be further investigated.

Acknowledgments

This research was financially supported by the Dutch Technology Foundation STW (grant no. 10703). The authors would like to thank Michelle Janssens, Hannah Scott, and Julie Bekaert for their technical assistance and the personnel at the DUBBLE beam line (BM26) at the ESRF for their support with the X-ray measurements. The ceramides were kindly provided by Evonik (Essen, Germany). The project was supported by COST (European Cooperation in Science and Technology).

Disclosure Statement

No competing financial interests exist.

References

1. Lampe, M.A., Burlingame, A.L., Whitney, J., Williams, M.L., Brown, B.E., Roitman, E., and Elias, P.M. Human stratum corneum lipids: characterization and regional variations. J Lipid Res **24,** 120, 1983.
2. Weerheim, A., and Ponec, M. Determination of stratum corneum lipid profile by tape stripping in combination with high-performance thin-layer chromatography. Arch Dermatol Res **293,** 191, 2001.
3. Wertz, P.W., Miethke, M.C., Long, S.A., Strauss, J.S., and Downing, D.T. The composition of the ceramides from human stratum corneum and from comedones. J Invest Dermatol **84,** 410, 1985.
4. Bouwstra, J.A., Gooris, G.S., van der Spek, J.A., and Bras, W. Structural investigations of human stratum corneum by small-angle X-ray scattering. J Invest Dermatol **97,** 1005, 1991.
5. Bouwstra, J.A., Gooris, G.S., Dubbelaar, F.E., and Ponec, M. Phase behavior of lipid mixtures based on human ceramides: coexistence of crystalline and liquid phases. J Lipid Res **42,** 1759, 2001.
6. Damien, F., and Boncheva, M. The extent of orthorhombic lipid phases in the stratum corneum determines the barrier efficiency of human skin *in vivo*. J Invest Dermatol **130,** 611, 2010.
7. Menon, G.K. New insights into skin structure: scratching the surface. Adv Drug Deliv Rev **54 Suppl 1,** S3, 2002.
8. de Brugerolle, A. SkinEthic Laboratories, a company devoted to develop and produce *in vitro* alternative methods to animal use. ALTEX **24,** 167, 2007.
9. El Ghalbzouri, A., Siamari, R., Willemze, R., and Ponec, M. Leiden reconstructed human epidermal model as a tool for the evaluation of the skin corrosion and irritation potential according to the ECVAM guidelines. Toxicol In Vitro **22,** 1311, 2008.
10. Hoffmann, S., and Hartung, T. Designing validation studies more efficiently according to the modular approach: retrospective analysis of the EPISKIN test for skin corrosion. Altern Lab Anim **34,** 177, 2006.
11. Kandarova, H., Liebsch, M., Spielmann, H., Genschow, E., Schmidt, E., Traue, D., Guest, R., Whittingham, A., Warren, N., Gamer, A.O., Remmele, M., Kaufmann, T., Wittmer, E., De, W.B., and Rosdy, M. Assessment of the human epidermis model SkinEthic RHE for *in vitro* skin corrosion testing of chemicals according to new OECD TG 431. Toxicol In Vitro **20,** 547, 2006.
12. Bell, E., Ehrlich, H.P., Buttle, D.J., and Nakatsuji, T. Living tissue formed *in vitro* and accepted as skin-equivalent tissue of full thickness. Science **211,** 1052, 1981.
13. Boyce, S.T., Christianson, D.J., and Hansbrough, J.F. Structure of a collagen-GAG dermal skin substitute optimized for cultured human epidermal keratinocytes. J Biomed Mater Res **22,** 939, 1988.

14. El Ghalbzouri, A., Lamme, E., and Ponec, M. Crucial role of fibroblasts in regulating epidermal morphogenesis. Cell Tissue Res **310,** 189, 2002.
15. Ponec, M., Gibbs, S., Weerheim, A., Kempenaar, J., Mulder, A., and Mommaas, A.M. Epidermal growth factor and temperature regulate keratinocyte differentiation. Arch Dermatol Res **289,** 317, 1997.
16. Hartung, T. Toxicology for the twenty-first century. Nature **460,** 208, 2009.
17. El Ghalbzouri, A., Commandeur, S., Rietveld, M.H., Mulder, A.A., and Willemze, R. Replacement of animal-derived collagen matrix by human fibroblast-derived dermal matrix for human skin equivalent products. Biomaterials **30,** 71, 2009.
18. Dickson, M.A., Hahn, W.C., Ino, Y., Ronfard, V., Wu, J.Y., Weinberg, R.A., Louis, D.N., Li, F.P., and Rheinwald, J.G. Human keratinocytes that express hTERT and also bypass a p16(INK4a)-enforced mechanism that limits life span become immortal yet retain normal growth and differentiation characteristics. Mol Cell Biol **20,** 1436, 2000.
19. Commandeur, S., Ho, S.H., de Gruijl, F.R., Willemze, R., Tensen, C.P., and El, G.A. Functional characterization of cancer-associated fibroblasts of human cutaneous squamous cell carcinoma. Exp Dermatol **20,** 737, 2011.
20. El Ghalbzouri, A., Gibbs, S., Lamme, E., Van Blitterswijk, C.A., and Ponec, M. Effect of fibroblasts on epidermal regeneration. Br J Dermatol **147,** 230, 2002.
21. de Jager, M., Groenink, W., Guivernau, R., Andersson, E., Angelova, N., Ponec, M., and Bouwstra, J. A novel *in vitro* percutaneous penetration model: evaluation of barrier properties with p-aminobenzoic acid and two of its derivatives. Pharm Res **23,** 951, 2006.
22. Thakoersing, V.S., Gooris, G.S., Mulder, A., Rietveld, M., El, G.A., and Bouwstra, J.A. Unraveling barrier properties of three different in-house human skin equivalents. Tissue Eng Part C Methods **18,** 1, 2012.
23. Thakoersing, V.S., van, S.J., Mulder, A.A., Vreeken, R.J., El, G.A., and Bouwstra, J.A. Increased presence of monounsaturated fatty acids in the stratum corneum of human skin equivalents. J Invest Dermatol **133,** 59, 2013.
24. Masukawa, Y., Narita, H., Shimizu, E., Kondo, N., Sugai, Y., Oba, T., Homma, R., Ishikawa, J., Takagi, Y., Kitahara, T., Takema, Y., and Kita, K. Characterization of overall ceramide species in human stratum corneum. J Lipid Res **49,** 1466, 2008.
25. Motta, S., Monti, M., Sesana, S., Caputo, R., Carelli, S., and Ghidoni, R. Ceramide composition of the psoriatic scale. Biochim Biophys Acta **1182,** 147, 1993.
26. van Smeden, J., Boiten, W.A., Hankemeier, T., Rissmann, R., Bouwstra, J.A., and Vreeken, R.J. Combined LC/MS-platform for analysis of all major stratum corneum lipids, and the profiling of skin substitutes. Biochim Biophys Acta **1841,** 70, 2013.
27. Groen, D., Gooris, G.S., and Bouwstra, J.A. Model membranes prepared with ceramide EOS, cholesterol and free fatty acids form a unique lamellar phase. Langmuir **26,** 4168, 2010.
28. Boelsma, E., Verhoeven, M.C., and Ponec, M. Reconstruction of a human skin equivalent using a spontaneously transformed keratinocyte cell line (HaCaT). J Invest Dermatol **112,** 489, 1999.
29. Maas-Szabowski, N., Starker, A., and Fusenig, N.E. Epidermal tissue regeneration and stromal interaction in HaCaT cells is initiated by TGF-alpha. J Cell Sci **116,** 2937, 2003.
30. Allen-Hoffmann, B.L., Schlosser, S.J., Ivarie, C.A., Sattler, C.A., Meisner, L.F., and O'Connor, S.L. Normal growth and differentiation in a spontaneously immortalized near-diploid human keratinocyte cell line, NIKS. J Invest Dermatol **114,** 444, 2000.
31. Rasmussen, C., Gratz, K., Liebel, F., Southall, M., Garay, M., Bhattacharyya, S., Simon, N., Vander, Z.M., Van, W.K., Pirnstill, J., Pirnstill, S., Comer, A., and Allen-Hoffmann, B.L. The StrataTest(R) human skin model, a consistent *in vitro* alternative for toxicological testing. Toxicol In Vitro **24,** 2021, 2010.
32. Ponec, M., Boelsma, E., Weerheim, A., Mulder, A., Bouwstra, J., and Mommaas, M. Lipid and ultrastructural characterization of reconstructed skin models. Int J Pharm **203,** 211, 2000.
33. de Jager, M., Groenink, W., van der Spek, J., Janmaat, C., Gooris, G., Ponec, M., and Bouwstra, J. Preparation and characterization of a stratum corneum substitute for *in vitro* percutaneous penetration studies. Biochim Biophys Acta **1758,** 636, 2006.

Address correspondence to:
Joke A. Bouwstra, PhD
Gorlaeus Laboratories
Department of Drug Delivery Technology
Leiden Academy Centre for Drug Research
Leiden University
Einsteinweg 55
Leiden 2333 CC
The Netherlands

E-mail: bouwstra@chem.leidenuniv.nl

Abdoelwaheb El Ghalbzouri, PhD
Department of Dermatology
Leiden University Medical Centre
P.O. Box 9600
Leiden 2300 RC
The Netherlands

E-mail: a.e.l.ghalbzouri@lumc.nl

Received: January 7, 2014
Accepted: April 25, 2014
Online Publication Date: August 1, 2014